DUAL-SCALE POROSITY ANALYSIS OF FIRED-CLAY BRICKS WITH DIFFERENT PORE-FORMING AGENTS AND CONCENTRATIONS

H. Kariem, Ch. Hellmich, J. Füssl

TU Wien Vienna University of Technology, Institute for Mechanics of Materials and Structures

Motivation

Masonry brick is a very well-known and long-standing building material. Originally mainly used for residential buildings with a small amount of storeys, its area of application has evolved towards larger buildings in recent years. In order to maintain this positive trend and to be competitive against other building materials, like concrete, a continuous optimization of this material is indispensable. One of the main challenges in this regard is a better understanding of the link between microstructure and the effective thermal conductivity of masonry bricks, which constitutes the high energy efficiency of this product. Different pore-forming agents in different concentrations are used in fired clay blocks to decrease the thermal conductivity by increasing its porosity. For this reason, determining the porosity, and its characteristics, is a crucial first step towards understanding the influence of the pore-forming agents and their concentrations on the thermal conductivity. A promising method to achieve this is micro-computed tomography, which is able to deliver quantitative as well as qualitative information on the micro- and macroporosity within the brick matrix, depending on pore-forming agents and their concentrations.

Materials & Methods

PORE-FORMING AGENTS

EPS	Paper sludge	Sawdust
10 %	10 %	10%
20 %	20 %	20%
	40 %	40%

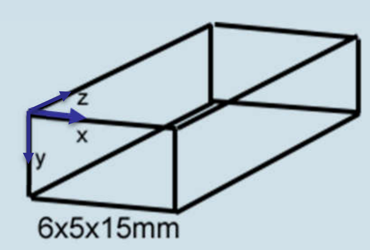

Extruded in x-direction
Fired at 880°C

X-RAY MICROTOMOGRAPHY (µCT)

Scan settings:

- 70 kVP, 114 µA, 300 ms
- Resulting voxel size: 6 x 6 x 6 µm
- 16 bit grey value range
- For reference: pure clay fired at 880°C & 1100°C also measured

MICROPOROSITY

The linear relationship between the x-ray attenuation coefficients and the grey values was statistically analyzed to obtain the coefficients a and b, which are photon energy ϵ dependent [3]:

$$\mu(\varepsilon) = a(\varepsilon) \times GV + b(\epsilon) \; .$$

The coefficients together with the most frequently recurring grey value were used to calculate the attenuation coefficient of each sample, $\mu_{Sample}(\varepsilon) = a(\varepsilon) \times GV_{Sample} + b(\epsilon)$.

The attenuation coefficient of each sample depends on the microporosity φ of the brick matrix and the attenuation coefficient of the completely dense brick matrix μ_{Matrix}^{NIST} as follows,

$$\mu_{Sample}(\varepsilon) = \mu_{Matrix}^{NIST}(1 \quad \varphi) + \mu_{Air}\varphi \; .$$

The chemical composition of the brick matrix was known, thus, it was possible to calculate μ_{Matrix}^{NIST} from the NIST database [4]. Based thereupon, the microporosity φ was computed for each sample,

$$\varphi = \frac{\mu_{Sample} - \mu_{Matrix}^{NIST}}{\mu_{Air} - \mu_{Matrix}^{NIST}} \; .$$

MACROPOROSITY

Samples with EPS and sawdust were segmented via the Otsu algorithm [1], threshold for paper sludge determined via a pore.

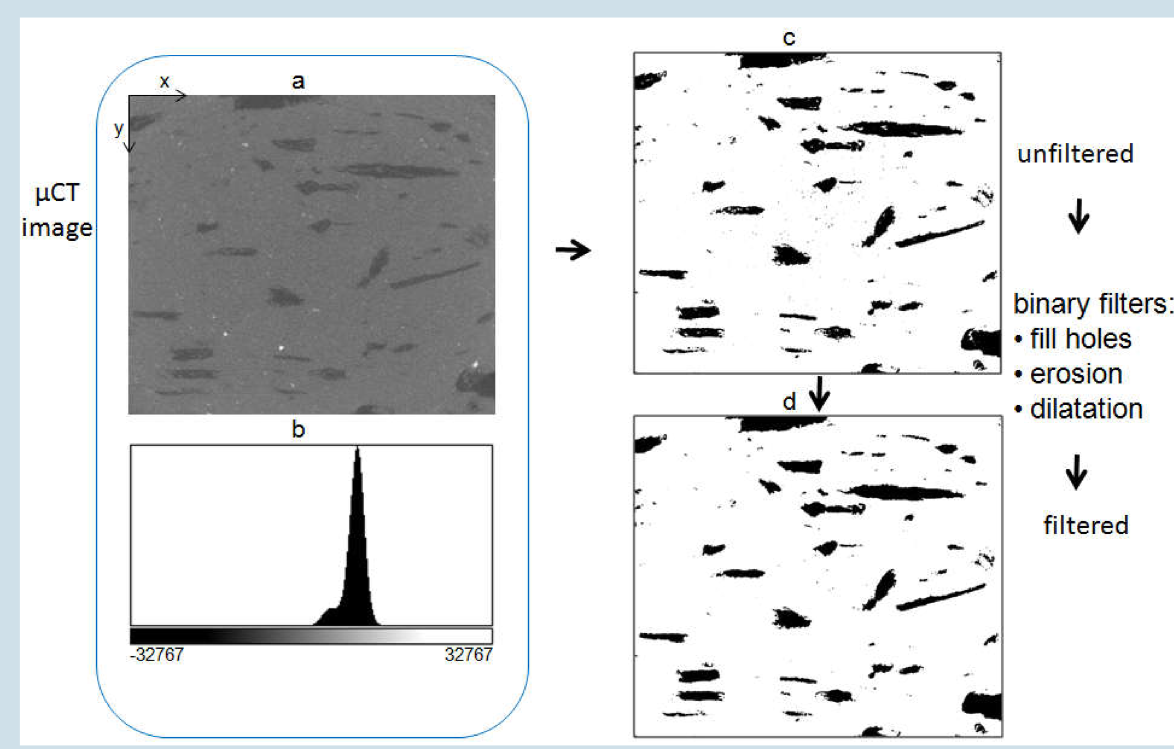

ImageJ [2] and various plug-ins were used to determine the volume and the orientation of the macropores.

Results & Discussion

MACROPORES

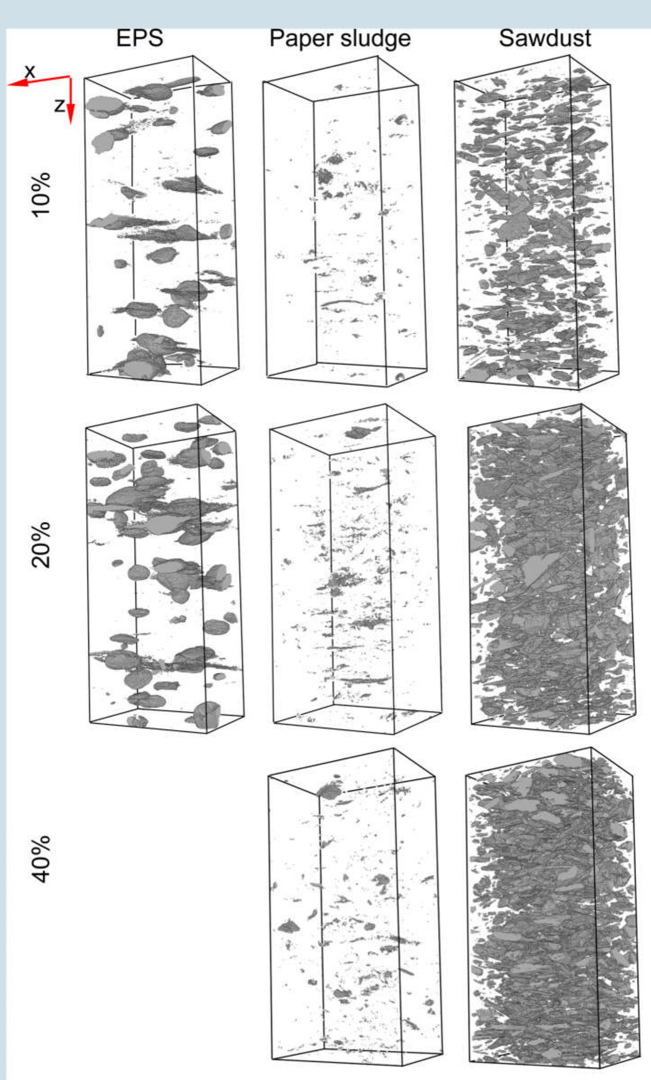

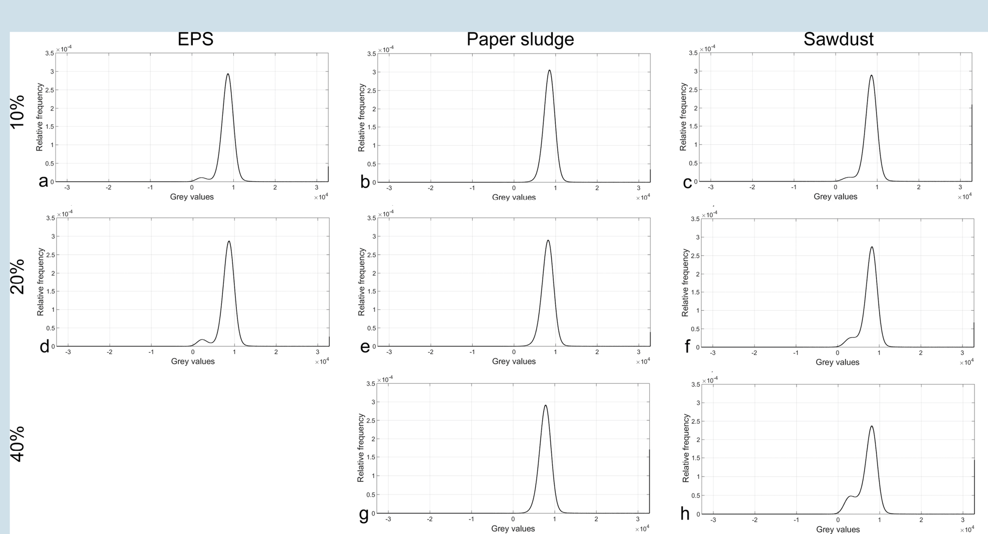

The grey value histograms of the samples with EPS and sawdust show a superposition of two distriubutions, the left one representing the macropores and the one with the higher grey value peak characterinzing the brick matrix. Samples with paper sludge do not show macropores, neither in the histogram, nor in the 3D segmentation. EPS causes bigger macropores, whereas the macroporosits is higher in samples with sawdust at the same concentration.

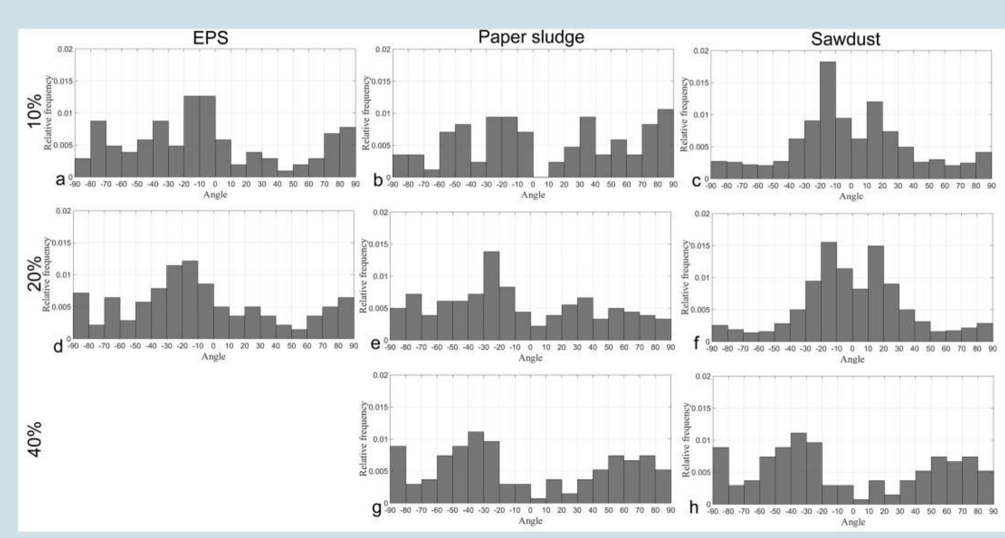

The angle between the extrusion direction and the macropores' major principal axis of inertia indicates the orientation of the macropores, which show a tendency to be aligned close to the extrusion direction in EPS and sawdust. It should be taken into account that the mouth piece of the extrusion press is most likely not perfectly aligned causing a deviation from the expected extrusion angle which should be 0.

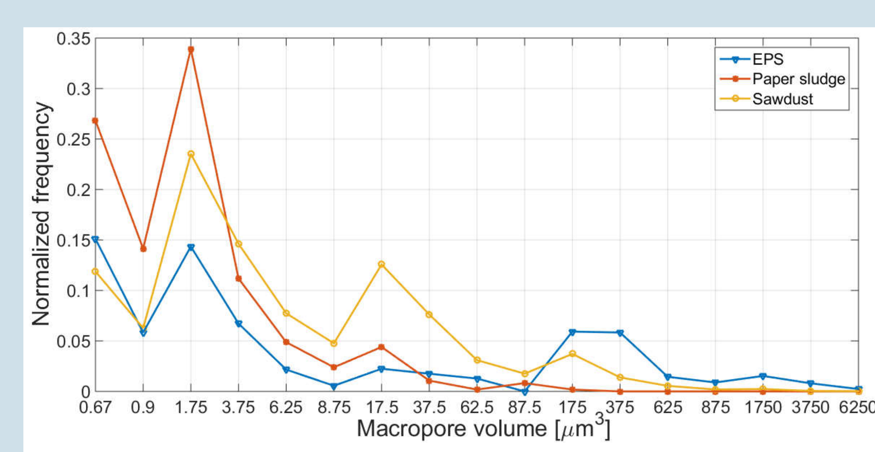

The relative frequency of each pore-forming agent was determined by computing the mean value of the relative frequency of all concentrations of each pore-forming agent. As illustrated, samples with EPS (blue) have more of the bigger macropores, which is also visible in the 3D segmentation image.

MICROPORES

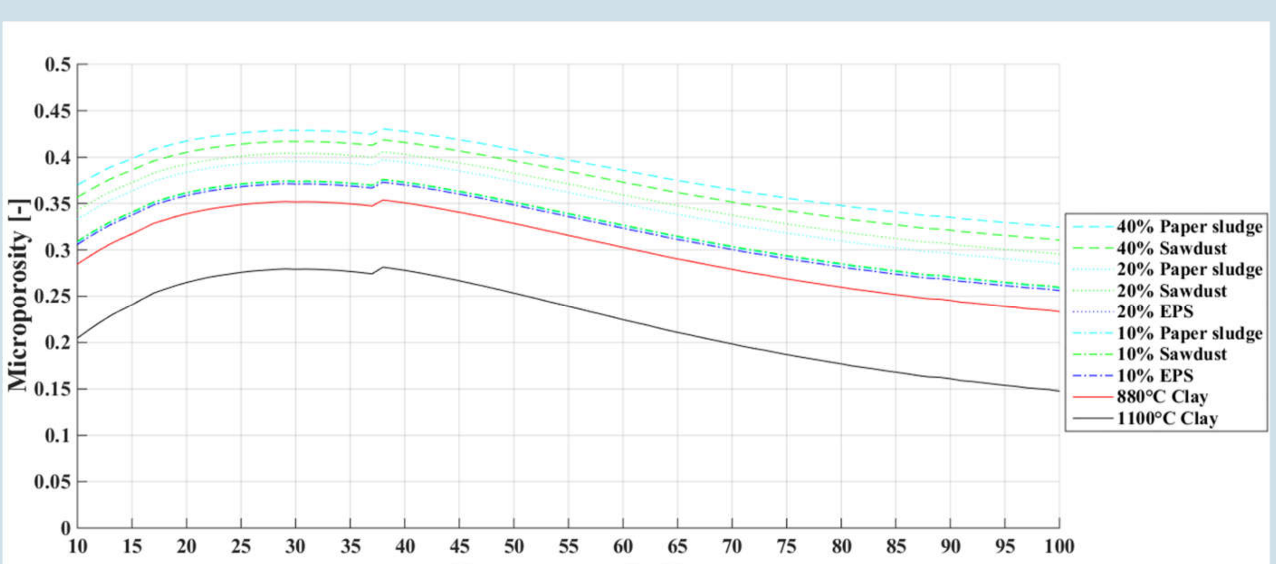

One single point, the maximum at 38 keV, relates the photon energy, the attenuation coefficient, and therefore the microporosity in a unique way which is the only physically admissible solution. Pure fired-clay have the lowest peak microporosity, whereas the sample with 40% paper sludge has the highest. An increase of the concentration of EPS does not influence the microporosity.

VALIDATION

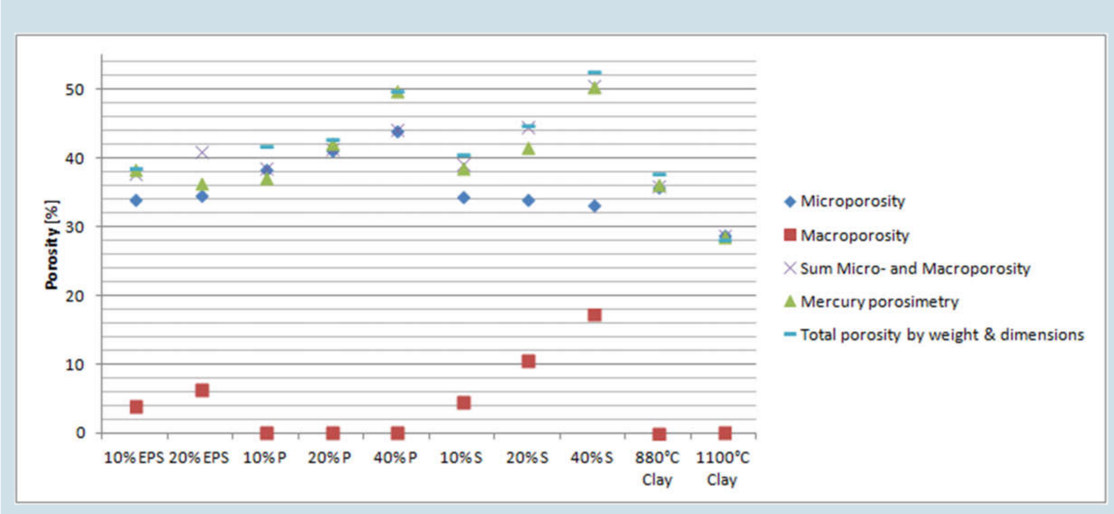

The sum of the mean microporosity and the macroporosity was compared to values obtained by mercury intrusion porosimetry and the total porosity calculated by weighing and mesuring the samples.

[1] N. Otsu. A threshold selection method from gray-level histograms. Systems, Man and Cybernetics, IEEE Transactions on, 9(1):62–66, Jan 1979.

[2] C.A. Schneider, W.S. Rasband, and K.W. Eliceiri. NIH image to ImageJ: 25 years of image analysis. Nat Meth, 9(7):671–675, July 2012.

[3] A. Czenek, R. Blanchard, A. Dejaco, O.E. Sigurjonsson, G. Örlygsson, P. Gargiulo, and C. Hellmich. Quantitative intravoxel analysis of microct-scanned resorbing ceramic biomaterials - perspectives for computer-aided biomaterial design. Journal of Materials Research, 29:2757–2772, 2014.

[4] J.H. Hubbell, S.M. Seltzer, Tables of X-Ray Mass Attenuation Coefficients and Mass Energy-Absorption Coefficients (version 1.4), [Online] available: http://physics.nist.gov/xaamdi, National Institute of Standards and Technology, Gaithersburg, 2004.A

33rd DANUBIA-ADRIA SYMPOSIUM on Advances in Experimental Mechanics, September 2016, Portorož, Slovenia